Hindawi
Journal of Advanced Transportation
Volume 2020, Article ID 8939621, 16 pages
https://doi.org/10.1155/2020/8939621

Research Article

Defining Highway Node Acceptance Capacity (HNAC): Theoretical Analysis and Data Simulation

Xingliang Liu, Jinliang Xu, Yaping Dong, Han Ru, and Zhihao Duan

Highway School, Chang'an University, Xi'an, China

Correspondence should be addressed to Jinliang Xu; xujinliang@chd.edu.cn

Received 30 August 2019; Revised 1 November 2019; Accepted 28 November 2019; Published 15 January 2020

Academic Editor: Alain Lambert

Copyright © 2020 Xingliang Liu et al. This is an open access article distributed under the Creative Commons Attribution License, which permits unrestricted use, distribution, and reproduction in any medium, provided the original work is properly cited.

A new concept of Highway Node Acceptance Capacity (HNAC) is proposed in this paper inspired by a field data observation. To understand HNAC in microscopic view, boundary condition of successful merging is found using car-following behaviours and lane-changing rules, which could also explain traffic oscillations. In macroscopic view, linear positive relationship between HNAC and background traffic volume is obtained based on moving bottleneck. To determine the explicit form of the relationship, data simulation considering car-following behaviours and traffic flow theory is used. In the results, the synchronization phenomenon of oscillation in on-ramp (with respect to main road) and intersected road is found. The explicit equation of HNAC is determined based on standard deviation and correlation coefficient analysis, and also proved to be accurate with model validation, which is helpful in studies related to propagation mechanism of traffic emergencies on highway network.

1. Introduction

In our previous work [1], traffic flow field data was collected on City Ring Road and Lianhuo Expressway, Xi'an. During the process of data collection, an interesting phenomenon was observed on Baqiao Interchange (K450 + 100 of Lianhuo Expressway, G30). Taking northbound traffic merging from City Ring Road to Lianhuo Expressway as an example (Figure 1), traffic condition of this highway node varies between morning and afternoon peak hours. In Figure 1(a), traffic condition at 8:30 a.m. was depicted. The traffic flow in downstream Lianhuo Expressway had traffic volume of 1830 veh/h ∗ l and density of 26 veh/km ∗ l, respectively. These two values in upstream City Ring Road were 465 veh/h ∗ l and 11 veh/km ∗ l, and merging volume of on-ramp was 330 veh/h ∗ l. It could be seen, all sections mentioned above were in free flow. This is mainly because during morning peak hour, people go into the city, which means going south. During afternoon peak hour, people go out northbound, which leads to a different situation. In Figure 1(b), traffic condition in downstream Lianhuo Expressway remained the same (volume of 1830 veh/h ∗ l and density of 26 veh/km ∗ l), but congestion was caused in upstream City Ring Road (volume of 272 veh/h∗l and density of 91 veh/km ∗ l) with the increase of merging traffic volume (665 veh/h ∗ l) in on-ramp.

Combining the example given above, some terms are defined here. The first term is "main road", defined as road section with traffic merging in of a highway interchange (like Lianhuo Expressway in the example). The second term is "intersected road", defined as road section with traffic diversion (like City Ring Road in the example). The third one is "highway node", which is a part of an interchange, consists of main road, intersected road and the on-ramp (with respect to main road) connecting them. Inspired by the phenomenon observed above, a problem could be presented here. If there was an oscillation downstream the main road, whether a specific upper limit exists, when exceeded by merging traffic volume, traffic flow of intersected road will be affected. This is crucial in research on propagation mechanism of traffic emergencies in highway network, which is very helpful to large scale evacuation and rescue. In 1995, Daganzo [2] provided a quite detailed study on traffic merging problem using cell transmission model. This is a classic research followed by many scholars, and there are still some works remaining to be done, to further improve this field. The method in his work mainly focused on the topological form of the junction and the logic between adjacent nodes, scilicet a partial mathematical method. Therefore, in consideration of practical application, some

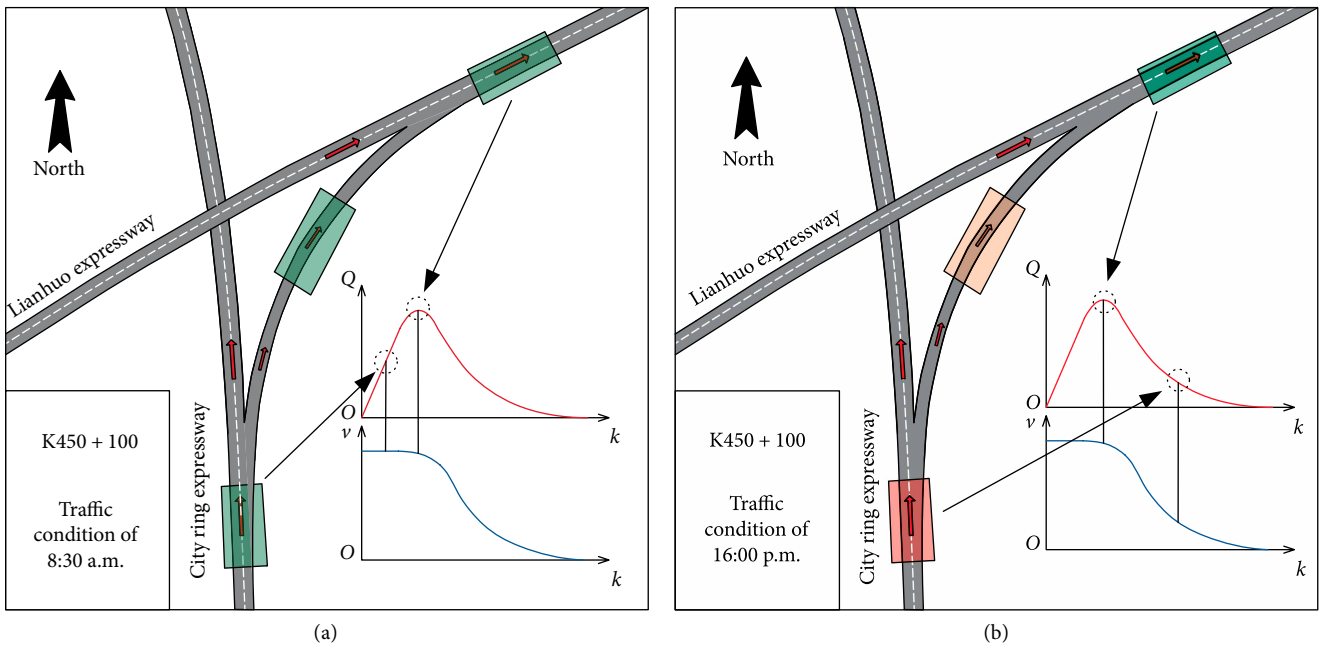

Figure 1: The phenomenon observed on Baqiao interchange. (The red arrow depicts moving directions of the vehicles, green rectangles depict free flow in certain sections, red rectangle depicts congested flow, and orange rectangle depicts the increase of traffic volume in on-ramp). (a) Traffic condition in Baqiao interchange at 8:30 a.m. (b) Traffic condition in Baqiao interchange at 16:00 p.m.

practical efforts could be done, including microscopic relationship among vehicles and traffic flow's physical characteristics in merging area, e.g.

Thus, to further ameliorate Daganzo's classic work, concept of Highway Node Acceptance Capacity (HNAC) is provided here. HNAC means the upper limit of traffic volume merging into the main road from the intersected road through the on-ramp. If this value was exceeded by merging volume, traffic flow in intersected road will be affected, showing obvious oscillations and further forming congestion. This parameter shares the same unit with traffic volume, scilicet veh/h · l. In microscopic view, study of HNAC is directly related to a specific vehicle's driving behaviour when merging into target lane in main road. Mentioning problems related to microscopic driving behaviour, car-following models and lane-changing rules become crucial because they are basic theories in this field, and they will be studied in Section 3. In macroscopic view, essence of studying HNAC is calculating the volume of successfully merging vehicles. Typically, a successful merging behaviour depends on enough large spacing between the leading vehicle and the follower in target lane, and the volume of large spacing is related to HNAC. In real traffic stream, spacing between adjacent vehicles is not homogeneous. The existence of slow vehicles will cause moving bottlenecks and reform the traffic stream. Therefore, in macroscopic study of HNAC, theories of moving bottleneck should be taken into consideration, and these contents will be studied in Section 4. Furthermore, literature review will be stated in Section 2. The process of data simulation is given in Section 5, and Section 6 provides the results, including the synchronization of oscillation in on-ramp and intersected road, standard deviation and correlation coefficient analysis, and the explicit equation of HNAC. Section 7 provides conclusions and some discussions.

2. Literature Review

As depicted in Section 1, HNAC was defined as the upper limit of traffic volume merging into main road through on-ramp. If this value was exceeded by merging volume, traffic flow in intersected road will be affected. This concept was firstly mentioned in Kerner's classical three phase traffic theory work in 2004 [3], by stating that "in free traffic of merging area, there might be random highway capacities which depend on the flow rate of on-ramp". This statement is related to the phenomenon observed in Section 1. However, unfortunately, in Kerner's abovementioned and following works [4–6], clear definition of HNAC and explicit formulas were not provided, either in other followers' works [7, 8].

This paper began with the definition of HNAC in Section 1. As depicted in previous part, car-following model is firstly considered. The car-following model developed by Newell [9] showed some significant importance and practicality in related works. This model clearly depicts the relationship between the leading vehicle's and the follower's moving condition. It implies the follower will change its velocity and spacing depends on the leader's driving condition with a small spatio-temporal hysteresis. Besides, compared to traditional car-following models, the dynamic process of acceleration and deceleration are considered as instantaneously completed. Therefore, this model showed some advantages in explicit traffic flow macroscopic modeling compared to those traditional ones [10–15]. Moreover, Newell's model showed the same accuracy and succinct formation with a different logic more suitable to modern traffic. Following theoretical and empirical studies of classic car-following model, relaxation phenomenon was discovered, showing that driver will accept shorter spacing and adjust it to more comfortable value in process of lane-changing or merging behaviour [16–20]. This concept and phenomenon

could be used as an assumption in microscopic modelling. Traffic oscillations and stop-and-go waves are common phenomena caused by lane-changing behaviours [21–23], which could be theoretically explained using car-following models. Therefore, this could be used as inspection standard in this paper. In Laval's related study [24], a parsimonious theory explaining the appearance and transformation of traffic oscillation was provided based on Newell's model, and, timid and aggressive driving behaviors were concluded, which could be used in macroscopic modelling of this paper. Set aside the theoretical researches, empirical data were also used in model formulation. In Chen's work [25], a behavioral car-following model was developed based on empirical trajectory data using NGSIM dataset, which revealed the dynamic behaviour profile of drivers experiencing traffic oscillations. The data characteristics in this work provided some references in data simulation. In recent works, the researches of car-following model were basically related to traffic control strategy and automated vehicle [26–28]. Among them, the work by Han provided a novel breakdown probability model based on extending Newell's model, and a traffic control method to obtain uniform spacing was developed considering low passing rate of connected automated vehicle technology.

Based on the concept of HNAC depicted in Section 1, lane-changing rule and model are problems which could not be ignored or avoided in microscopic modelling in this work. The driver's decision to change lanes derived from his or her answers to three questions, whether it is possible, necessary, and desirable to change lanes [29]. In his work, structure of the driver's decision process before changing lanes was modelled. It has been regarded as a procedural and hierarchy basis in lane-changing models. Following lane-changing rules, the method of cellular automata was used in model formation [30, 31]. In anterior work, effects of various rules of lane-changing on characters of traffic flow were studied. The results showed that most efficient rules would be those allow fast vehicles to travel as fast as possible without sacrificing the total throughput. In the latter work, a general scheme of lane-changing rules was proposed based on summary of different approaches. In this work, Wagner's gap rules [32] were developed and realistic lane-changing rules were obtained. In the researches of lane-changing model, data simulation was frequently used. The classic study by Hidas [33] should be noticed. The detailed and inspirational lane-changing and merging algorithms were presented in this work, indicating that forced and cooperative lane changing are essential, which could produce realistic volume-velocity relationships during congested conditions. In 2006, a statement that lane-changing behaviours were strictly related to moving bottleneck and traffic volume reduction was proved by Laval [34]. In this work, the mechanism mentioned above was explained by a model that tracks lane-changing vehicles precisely. Besides, two phenomena previously thought to be unrelated were combined by this simplified parameters model, passing rate drop of bottleneck at the beginning of congestion, and the relationship between moving bottleneck velocity and its capacity. Safety criteria should be regarded as a boundary condition in lane-changing models. In Kesting's work [35], a general lane-changing model was proposed for discretionary and mandatory lane-changing behaviours. The essence of safety criteria was explored in his paper, in other words, the merging vehicle should keep safe distance with the leader and the follower in targeted lane.

As depicted in previous part, the theories of moving bottleneck could provide a reasonable explanation of vehicle distribution characters in real traffic flow. This phenomenon was systematically studied by Gazis [36], and the widely used model was developed by Newell [9]. In their work, the definition of moving bottleneck was given, and the model of passing rate, queue behaviour, moving queue growth rate were also provided. These results were widely used and developed in related researches [28, 37–39].

3. Microscopic Modelling of HNAC

In microscopic perspective, research on HNAC could be related to specific situation stated as below. Imagine that, a vehicle traveling from on-ramp at a stable velocity, having the demand to enter the main road. However, the spacing between the leading vehicle and following vehicle in target lane does not satisfy the microscopic lane changing condition. Therefore, the vehicle ready to enter the main road has to decelerate and wait for a proper chance. This situation might lead to congestion in on-ramp and further affects the traffic condition in intersected road. This situation could be interpreted as: the volume sent by on-ramp exceeds the HNAC of the main road.

From the simplified description in previous context, the microscopic modelling should consist of two important parts, car-following behaviour and lane-changing condition.

3.1. Car-Following Behavior. For analytical tractability, vehicles are assumed to follow the classic car-following model by Newell [9]. This model provides two crucial contents, the relationship between the leading vehicle and following vehicle's trajectory in time and space, and, the relationship between a vehicle's spacing and velocity. This model formed the basic laws in car-following research areas, adopted and developed by many researchers [18–20, 24, 25, 28].

In Newell's model, highway is treated as a homogeneous carrier, and spacing is linear related to travel velocity. When the leading vehicle changed its operation velocity, the follower would change its speed according to the leader's, but there is a hysteresis that exists in time and space. This relationship could be depicted in Figure 2.

As depicted in left side of Figure 2(a), the trajectories of leading vehicle and the follower's are represented by $x_{n-1}(t)$ and $x_n(t)$ respectively. At a time point, the leader accelerated from v_{n-1} to v'_{n-1} ($v_{n-1} < v'_{n-1}$). However, the follower did not change its velocity immediately. Instead, after a time period τ_n, when the spacing of the follower increased from S_n to S'_n, the follower also accelerated to v'_n. The parameters τ_n and δ_n related to hysteresis phenomenon are independent from v_n, they depend on the driver himself. The trajectory in car-following model and the relationship between spacing and velocity depicted in Figure 2 could be expressed as below.

$$S_n = S_n + v_n \tau_n, \tag{1}$$

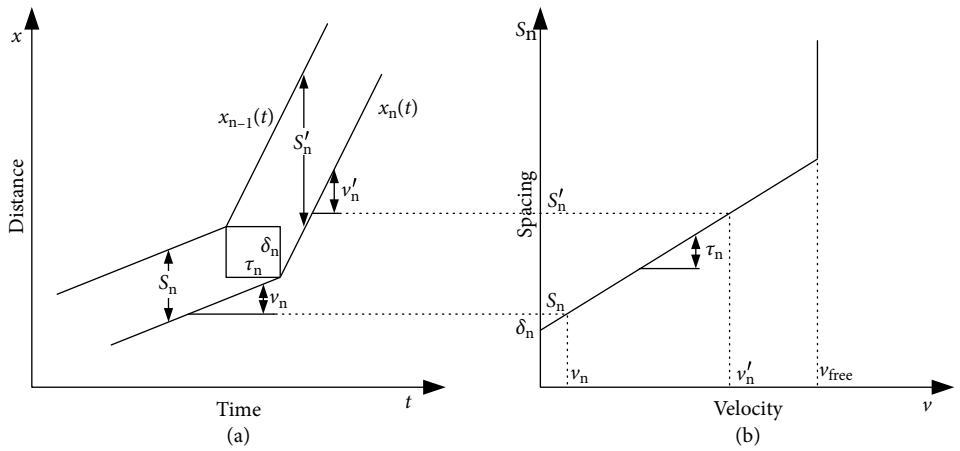

Figure 2: Schematic diagram of Newell's car-following model. (a) The trajectories of leading vehicle and the follower's. (b) The relationship between spacing and velocity in Newell's model.

$$x_n(t+\tau_n) = x_{n-1}(t) - \delta_n. \tag{2}$$

In the two equations shown above, δ_n could be defined as the spacing in totally congested traffic, and τ_n could be defined as the time consumption by which the kinematic-wave travels a distance of δ_n [37]. As depicted in Figure 2(b), there is a limitation $v_n \in [0, v_{free}]$, which means equation (1) only established in congested traffic flow (the right side of volume-density curve). To a steady traffic flow, all of the vehicles travel at nearly the same velocity v, then we get:

$$\begin{aligned} \overline{S} &= \overline{\delta} + v\overline{\tau}, \\ \overline{\tau} &= \frac{1}{n}\sum_{k=1}^{n}\tau_k, \quad \overline{\delta} = \frac{1}{n}\sum_{k=1}^{n}\delta_k. \end{aligned} \tag{3}$$

It should be noticed, in real restricted traffic flow, the spacing varied due to the personality of the drivers. Aggressive drivers tend to choose smaller spacing (τ_n, δ_n) and vice versa, timid drivers tend to have loose spacing. It should be noted, car-following model is used in restricted flow, in which the follower should change its running velocity and spacing according to the leader's. In traditional traffic flow theory, there is a boundary concentration k_b between restricted flow and free flow [40]. In free flow condition, the driver operates in free flow velocity v_{free}, and maintains the spacing larger than $S_{n,free} = \delta_n + v_{free}\tau_n$ owning to the low concentration. When the concentration equals to k_b, the traffic flow is about to enter the restricted condition. At this moment, the driver in free flow gets its smallest spacing equal to $S_{n,free}$.

3.2. Microscopic Modelling Based on Lane-Changing Rules. As described in previous part, the microscopic modelling of HNAC could be transferred to a problem related to lane-changing rules. To be precise, to find a boundary spacing between two adjacent vehicles in targeted lane of the main road for the vehicle from on-ramp at a specific velocity to enter.

Lane-changing rules are first developed by P. G. Gipps in 1985 [29], with the perfections of the followers [21, 30, 31, 33, 35]. It is commonly accepted that after the lane-changing vehicle enters the target lane, it should keep a "safe distance" with the leading vehicle and the following one. It is known that the "safe distance", referred to as spacing, is related to operation velocity of the vehicle. Therefore, equation (3) should be cooperated in microscopic modelling.

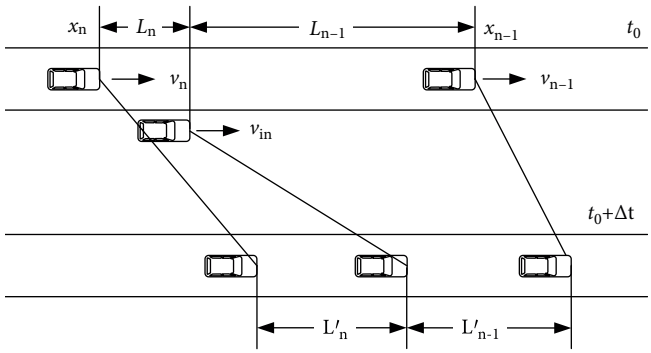

Figure 3: Schematic diagram of Lane-changing process.

To simplify the modelling process, assuming that merging vehicle completes its lane changing process in a short period without acceleration or deceleration, soon after it enters the target lane, the vehicle will adjust its velocity according to the leader's driving condition, and the follower will also adjust its velocity according to the lane-changing vehicle's driving condition. This process is depicted in Figure 3.

At time point t_0, a vehicle traveling from on-ramp with velocity v_{in} shows up at any position beside the target lane. In target lane, the follower at position x_n is traveling at velocity v_n, and the leader at position x_{n-1} is traveling at velocity v_{n-1}. At t_0, the distance between each vehicle are L_n and L_{n-1}. At time point $t_0 + \Delta t$, the vehicle has just finished its lane-changing process. The distance between each vehicle are L'_n and L'_{n-1}. In this process, L'_{n-1} and L'_n could be calculated using Equations (4) and (5).

$$L'_{n-1} = L_{n-1} - \Delta t(v_{in} - v_{n-1}), \tag{4}$$

$$L'_n = L_n - \Delta t(v_n - v_{in}). \tag{5}$$

With the lane-changing rules in the 2nd paragraph of this section, and cooperating equation (3), the boundary spacing L_{limit} between two adjacent vehicles in targeted lane could be obtained.

$$L'_{n-1} \geq S_{\text{in}} = \overline{\delta} + \overline{\tau} \cdot v_{\text{in}}, \tag{6}$$

$$L'_{n} \geq S_{n} = \overline{\delta} + \overline{\tau} \cdot v_{n}, \tag{7}$$

$$L_{\text{limit}} = 2\overline{\delta} - \Delta t(v_{n-1} - v_{n}) + \overline{\tau}(v_{\text{in}} + v_{n}). \tag{8}$$

The modelling of HNAC is strongly related to the boundary spacing L_{limit}. Imaging that, the vehicle traveling from the on-ramp is ready to merge into the target lane in main road. However, the spacing of the traffic flow in target lane of the main road is smaller than L_{limit}, meaning there is no chance for this vehicle to merge in. Therefore, this vehicle from on-ramp has to slow down or even stop to wait a proper chance. This is the situation for one single merging vehicle, just like an unsuccessful interpolation of two gearwheels. In real traffic condition, merging traffic from the on-ramp is continuous, indicating that if the volume of spacing satisfied L_{limit} in main road traffic flow is not enough for the merging traffic volume from on-ramp to consume, a congestion might form on the on-ramp and further affect the intersected road.

It should be noticed that the merging process varies depending on different relationships among v_n, v_{n-1}, and v_{in}. To further study, six situations are established and the merging process in each situation is shown in Figure 4.

In all of the 6 situations, the merging vehicle doesn't need to change its velocity only in situation (2). When $v_{n-1} > v_{\text{in}} > v_n$, the distances among three vehicles will get larger, and this is the most idealized condition. From situation (1) and (4), when $v_{\text{in}} > v_n$, whatever the relationship between v_n and v_{n-1}, the driver has to change the velocity according to the leader, which means the merging vehicle will join the downstream platoon and shows no affection on upstream traffic. From situation (3), (5), and (6), when $v_{\text{in}} < v_n$, it is important to notice that an oscillation shows up with a transmission speed equal to $\overline{\delta}/\overline{\tau}$, which means the merging vehicle forms a moving bottleneck that affects the upstream traffic. Besides, it also proved that the lane-changing behaviour will lead to some traffic oscillations, that is, if intersected road is affected when the transferred volume exceeds HNAC, it is important to distinguish the affection of oscillations and from the on-ramp, scilicet HNAC.

4. Macroscopic Modelling of HNAC

In this part, the range of macroscopic study should be firstly defined. Microscopic study mentioned in Section 3 depicted a research scope concentrate on single vehicle's moving condition. Compared to concept of microscopic study, macroscopic modeling concentrates on traffic flow in a certain highway node, especially the traffic flow in main road. In Section 3, $\overline{\delta}$ and $\overline{\tau}$ were adopted as average values, which means L_{limit} only depends on velocity. If a spacing in target lane is larger than L_{limit}, which means that it's effective for a merging vehicle to enter the main road at v_{in}, then this spacing could be called an "effective spacing" (ES). The essence of HNAC macroscopic modelling is to calculate the volume of ES passed the entrance in a time unit, and determine the relationship between ES number (ESN) and traffic volume Q in main road.

4.1. HNAC Macroscopic Modelling in Congested Flow. As depicted in previous part, congested flow refers to the right side of volume-density curve. In this situation, the velocity of each vehicle in traffic flow is assumed to be the same, v. Then L_{limit} could be reformed as below.

$$\begin{aligned} L_{\text{limit}} &= 2\overline{\delta} - \Delta t(v_{n-1} - v_{n}) + \overline{\tau}(v_{\text{in}} + v_{n}) \\ &= S_{\text{in}} + \overline{\delta} + \overline{\tau}\text{v} = S_{\text{in}} + S(v). \end{aligned} \tag{9}$$

From equation (9), $L_{\text{limit}} = S_{\text{in}} + S(v) > S(v)$, which means there is no chance for merging vehicle to enter the main road, and this is obviously unrealistic. The truth is, in congested flow, even the velocity is treated as equal, the spacing differs from each other due to the variance of δ and τ. To aggressive drivers, they tend to choose smaller δ and τ, as for timid ones, they tend to choose larger values [24], which could be expressed as below.

$$S_{\text{agg}} = \delta_{\text{agg}} + \delta_{\text{agg}} v < L_{\text{limit}}, \tag{10}$$

$$S_{\text{tim}} = \delta_{\text{tim}} + \delta_{\text{tim}} v > L_{\text{limit}}. \tag{11}$$

Therefore, assuming a vehicle platoon's volume equals to n. Among them, the ratio of ESN derived from timid driver is assumed as p, then the length of the vehicle platoon could be calculated using equations (12). The time consumption and traffic volume of passing a specific entrance could be calculated by equations (13) and (14).

$$L = (n-1)S(v) = (n-1)\left(\overline{\delta} + \overline{\tau}\text{v}\right), \tag{12}$$

$$T = \frac{L}{v}, \tag{13}$$

$$Q = \frac{n}{T} = \frac{\text{nv}}{L}. \tag{14}$$

Then, combining equations (12)–(14), the ESN could be expressed as below,

$$\text{ESN} = p(n-1) = p(\text{QT} - 1) = p\left(\frac{\text{QL}}{v} - 1\right), \tag{15}$$

which means ESN is linear positive correlated to traffic volume. But, it should be clarified that the model given above is an ideal situation. Here provides an example to show the reality in some degree, shown in Figure 5. A platoon consists of four vehicles is going to pass an entrance located at $x = 0$, and they are all operated by timid drivers with velocity v. The initial spacing $S_{\text{tim}} = L_{\text{limit}}$. At the time point $t = t_0$, a merging vehicle from on-ramp begins entering the target lane, and adjusts its velocity from a lower value to v. In order to keep the spacing S_{tim}, the three followers have to decelerate and lead to an oscil-

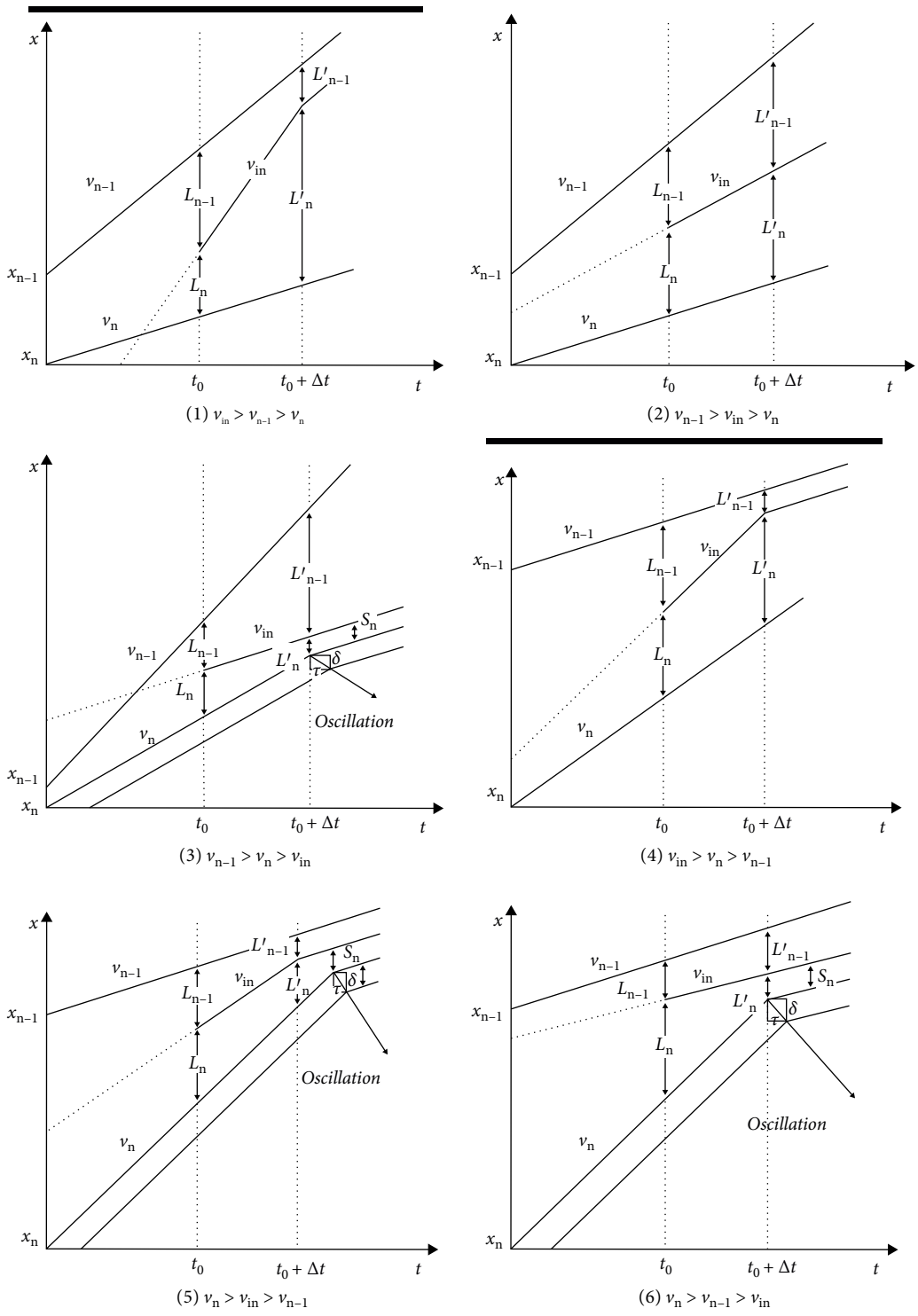

Figure 4: Schematic diagram of the Merging process in different situations.

lation. The actual spacing passing the entrance were S_1, S_2, and S_3. From the figure depicted this process given below, it is easy to conclude that $S_1 = S_3 = L_{limit}$, $S_2 < L_{limit}$. Therefore, the actual ESN turns from three to two. That is to say, in real traffic flow, the actual ESN will be lower than the value given by equation (15).

4.2. HNAC Macroscopic Modelling in Free Flow. The vehicle distribution character in free flow is different from congested flow. Due to the existence of moving bottleneck, it is unreasonable to regard every vehicle's velocity as free flow speed v_{free}. In the part without moving bottleneck, each vehicle travels with velocity v_{free}. Taking the description in last part

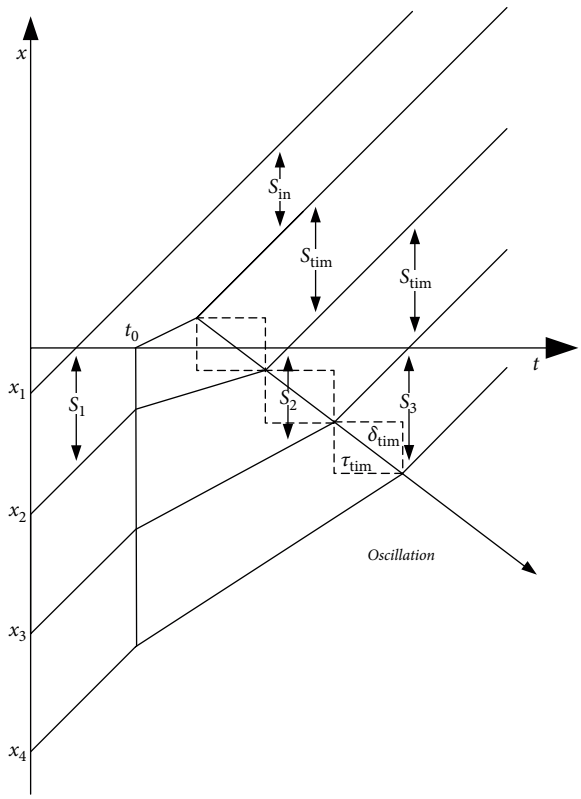

Figure 5: Schematic diagram of the real traffic ESN.

of Section 3.1, the distance between adjacent vehicles L_n and L_{limit} could be expressed as below.

$$L_n > S_{free} = \overline{\delta} + \overline{\tau} v_{free}, \tag{16}$$

$$L_{limit} = S_{in} + \overline{\delta} + \overline{\tau} v_{free} = S_{in} + S_{free}. \tag{17}$$

In the part of a stable moving bottleneck, the traffic condition becomes complex. Moving bottleneck is caused by slow moving vehicles in free traffic flow. Free running vehicles have the demand to pass the slow one (moving bottleneck), and a queue would form behind the bottleneck until it reached a stable length. The traffic characteristics in moving bottleneck could be expressed by Figure 6 [36].

In queue region, it could be seen that the travel velocity and concentration in all of the lanes are nearly the same, expressed as v_b and k_b. While in downstream, operation speed basically equals to v_{free}. However, concentration k_{blo} in blocked lane is smaller than k_{free} in upstream region, concentration k_{un} in unblocked lane is smaller than k_{blo}. This could be interpreted as the vehicles escaped from queue region didnot spread in each lane in average.

Moreover, when getting back to the calculation of HNAC, the traffic volume escaped from queue region and entered the target lane should be taken into consideration. When the capacity of downstream road is known as C, the portion of volume enters the target lane is q, then the volume referred in previous q_r could be calculated as below [38].

$$q_r = Cq\left(1 - \frac{v_b}{v_{free}}\right). \tag{18}$$

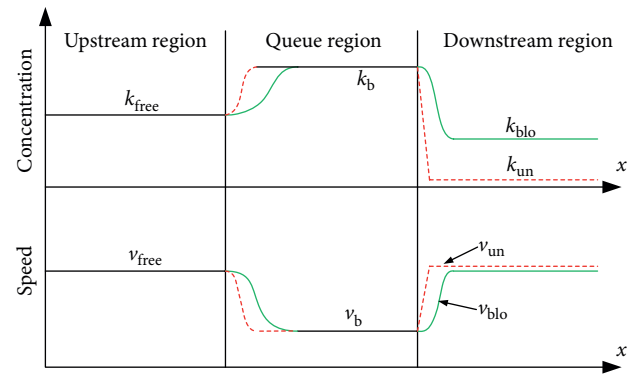

Figure 6: Schematic diagram of the traffic characteristics in moving bottleneck.

In moving bottleneck region, $v_b < v_{free}$, then we have:

$$S(v_b) < S(v_{free}) < L_{limit} = S_{in} + S_{free}. \tag{19}$$

For simplification, discrepancy among the drivers is ignored. Therefore, it is reasonable to assume that ES only exists in the part of free driving. In the part of moving bottleneck, every spacing does not satisfy the merging condition. Assuming that the length of a stable moving bottleneck is L_b, the distance between the leading vehicle and the entrance is L_{free}. In a time period T, the last vehicle in moving bottleneck passed the entrance, and the background traffic flow parameters counted by an observer on the entrance is average volume $\overline{Q}$, average speed $\overline{v}$, average concentration $\overline{k}$. The parameters in free flow part and bottleneck part are represented by (v_{free}, k_{free}) and (v_b, k_b), respectively. Then ESN could be calculated by equation (20).

$$ESN = L_{free} k_{free} + Tq_r - 2. \tag{20}$$

In equation (20), $L_{free} k_{free}$ represents the vehicle number in free flow part, and Tq_r stands for vehicle number escaping from queue region and it entered the target lane. It is known, $L_b + L_{free} = \left(\overline{Q}T/k\right)$, combined with equation (18), we have:

$$ESN = L_{free} k_{free} + \frac{\overline{Q}T}{\overline{k}} \cdot \frac{Cq(v_{free} - v_b)}{v_{free} v_b}. \tag{21}$$

By equation (21), we can draw the conclusion that ESN is linear positive correlated to traffic volume and linear inversely proportional to traffic concentration.

5. Data Simulation

According to results obtained from Section 4.1 and 4.2, HNAC (ESN) is theoretically linear correlated to the background traffic volume of the main road. Besides, from analysis in the last part of Section 4.1 and equation (21), it is known that the real ESN in free flow is lower than the value calculated by equation (15), and the equality relationship is only obtained in congested traffic flow. Moreover, in equation (21), ESN could not be directly obtained because the values of parameters L_{free}, T, q, and v_b are undetermined.

To determine L_{free}, T, q, and v_b based on theoretical analysis is unrealistic and unworthy because they are assumed to be random. Therefore, to obtain the explicit form of equation (21), method of data simulation is adopted in this paper. In the process of data simulation, traffic model in our previous work [1, 40] is adopted, shown in equation (22), depicts the relationship among traffic volume V, concentration k and heavy vehicle mixing ration r.

$$V = f(k, r) = \frac{v_f}{\left(1 + \exp\left(x - k_t/-0.23 * r + 1.243\right)\right)^{0.0025k_m * -0.1538}}. \quad (22)$$

In this paper, the simulation platform VISSIM is adopted, which provides a high level of details and flexibility in highway design, vehicle performance and driver's behaviours. According to the user manual, three detailed aspects should be noticed in the process of building HNAC (ESN) simulation model [41]: vehicle movement at highway merging area, velocity adjusting area in highway on-ramp, and car-following behaviours.

In aspect of vehicle movement in highway merging area, routes of the merging vehicles from on-ramp should extend beyond the whole weaving area, which ensures that vehicles from highway on-ramp successfully complete their merging movement. In consideration of second aspect, a velocity adjusting area should be defined in simulation model to provide a space for the drivers to decelerate or accelerate to v_{in} when approaching the entrance to identify if a suitable gap (ES) was available in target lane. The length of this area adopted in simulation model is 30 m setup 10 m upstream of the entrance according to previous field data collection. Taking car-following behaviors, Wiedemann 99 model is adopted since it is suitable for interurban traffic, and the microscopic parameters related to driving behaviours are adopted in Table 1 [42], based on the large amount field data collected on West 3rd Ring Expressway, Beijing. Simulation model derived from the contents above is shown in Figure 7.

As depicted in previous contents, the purpose of data simulation is to obtain the explicit form of HNAC (ESN). Considering the concept of HNAC in Section 1, the manifestation of exceeding HNAC is an oscillation in intersected road conducted through on-ramp from the main road. Therefore, a detector should be deployed upstream from the ramp in intersected road to observe the traffic condition affected by exceeding HNAC, shown in the below part of Figure 7. In order to catch the oscillation, the background traffic input in intersected road should possess a relatively lower robustness, which is the demarcation point of free flow and congested flow (v_{inter} = 81.8 km/h, k_{inter} = 33 veh/km ∗ l, Q_{inter} = 2699 veh/h ∗ l) [1].

In the upper part of Figure 7, a detector is deployed downstream at the terminal of the ramp to supervise the traffic condition of the main road. Besides, as depicted in Section 4.2, HNAC (ESN) is linearly related to traffic volume in main road. Therefore, the background traffic input in the main road should vary in traffic volume and heavy vehicle mixing ratio. The specific values of k_{main}, v_{main}, and Q_{main} are shown in Table 2 (the concentration varies regularly, the volume and speed varies according to equation (22). As depicted in the last part of Section 3.2, the oscillation derived from exceeding HNAC shows synchronization with the traffic condition in on-ramp. Therefore, in Figure 7, a detector is also deployed to observe the traffic condition in on-ramp. To find HNAC, the merging traffic volume also varies, shown in Table 2.

Table 1: Microscopic parameters related to driving behaviors.

	Microscopic parameters simulation model	Value
P1	Minimum headway (m)	1.75
P2	Maximum deceleration (m/s^2)	−4.4
P3	Reduction factor of desired safety distance (m)	0.67
P4	Maximum look ahead distance (m)	246.49
P5	Average standstill distance (m)	1.11
P6	Additive part of desired safety distance	1.81
P7	Multiple part of desired safety distance	3.05

6. Results

6.1. The Synchronization of Oscillation in On-Ramp and Intersected Road. To make the simulation feasible, number of simulation groups should be relatively limited. Therefore, 11 large groups were divided according to heavy vehicle mixing ratio r, seen in Table 2, r = 5% was settled as step distance. In each large group, 10 sub-groups were divided according to concentration in main road, based on step distance of Δk_{main} = 4. So, the concentration in main road varied from relatively free flow to congested flow, representing the most common traffic conditions in daily life. T aking the data from four groups when r = 10% as examples, which numbered 10–2–1 (v_{main} = 54.9 km/h, k_{main} = 34 veh/km ∗ l, Q_{main} = 1868 veh/h ∗ l, Q_{in} = 100 veh/h ∗ l), 10–2–3 (v_{main} = 54.9 km/h, k_{main} = 34 veh/km ∗ l, Q_{main} = 1868 veh/h ∗ l, Q_{in} = 300 veh/h ∗ l), 10–2–7 (v_{main} = 54.9 km/h, k_{main} = 34 veh/km ∗ l, Q_{main} = 1868 veh/h ∗ l, Q_{in} = 700 veh/h ∗ l), 10–2–10 (v_{main} = 54.9 km/h, k_{main} = 34 veh/km ∗ l, Q_{main} = 1868 veh/h ∗ l, Q_{in} = 1000 veh/h ∗ l), respectively. The synchronization of oscillation in on-ramp and intersected road could be easily observed in Figure 8.

The figures depicted in Figure 8 come from a simulation group consisting of 18 simulation tests, in which the merging traffic volume Q_{in} varies from 100 veh/h ∗ l to 1800 veh/h ∗ l (ΔQ_{in} = 100 veh/h ∗ l). In Figure 8(a), Q_{in} = 100 veh/h ∗ l, which is a relatively very low volume, caused no oscillation in both the intersected road and on-ramp. In Figure 8(b), Q_{in} = 300 veh/h ∗ l, higher than previous volume, caused some oscillations in intersected road. It should be noticed that there is no oscillation that appears in on-ramp, considering the analysis in the last part of Section 3.2, this is due to the lane-changing behaviours in intersected road. In Figure 8(c), Q_{in} = 700 veh/h ∗ l, there is also no oscillation appears in on-ramp. But the frequency of oscillation in the intersected road is obviously larger than that in Figure 8(b), which means the increasing number of lane-changing behaviours lead to severe velocity dispersion in the intersected road. In Figure 8(d), Q_{in} = 1000 veh/h ∗ l, when $T \in [0\,s, 1500\,s]$, the traffic condition in intersected road and on-ramp showed the

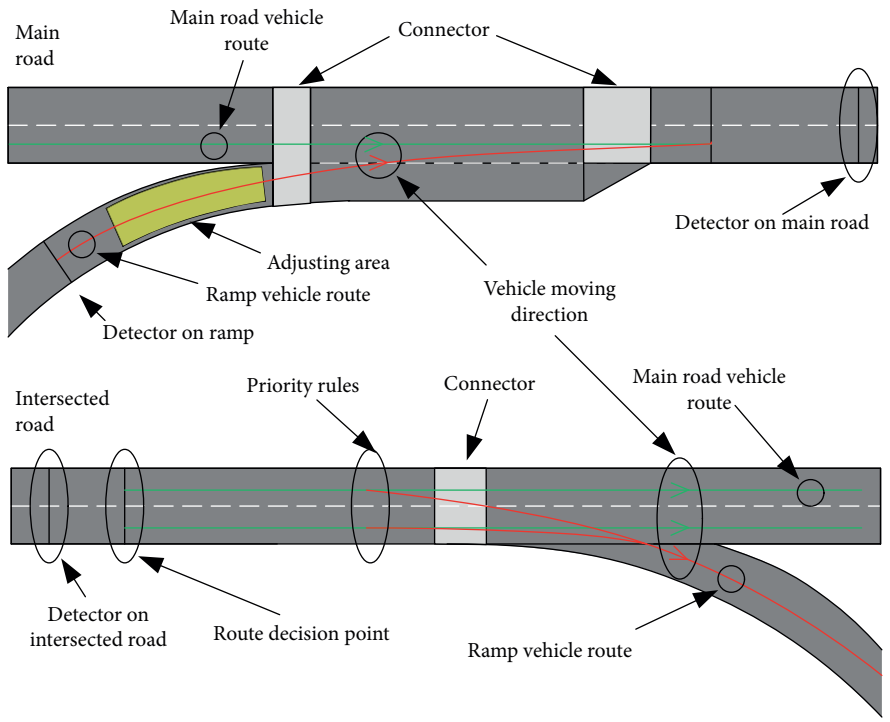

Figure 7: VISSIM simulation model.

Table 2: Background traffic input on main road and the merging traffic volume.

Heavy vehicle mixing ratio r (%)	Concentration on main road k_{main} (veh/km ∗ l)	Concentration step Δk_{main} (veh/km ∗ l)	Merging traffic volume Q_{in} (veh/h ∗ l)	Merging traffic volume step ΔQ_{in} (veh/h ∗ l)
0	33–69	4	100–50%Q_{main}	100
5	31–67	4	100–50%Q_{main}	100
10	30–66	4	100–50%Q_{main}	100
15	29–65	4	100–50%Q_{main}	100
20	28–64	4	100–50%Q_{main}	100
25	26–62	4	100–50%Q_{main}	100
30	25–61	4	100–50%Q_{main}	100
35	23–59	4	100–50%Q_{main}	100
40	22–58	4	100–50%Q_{main}	100
45	21–57	4	100–50%Q_{main}	100
50	20–56	4	100–50%Q_{main}	100

same characters in Figures 8(b) and 8(c). When coming to $T \in [1500\text{ s}, 3500\text{ s}]$, it is important to notice that velocity collapse and velocity synchronization appeared in both the intersected road and on-ramp, meaning that the merging traffic volume exceeded HNAC, leading oscillations conducting to intersected road through on-ramp.

In all of the 18 simulation tests in the group of $v_{main} = 54.9$ km/h, $k_{main} = 34$ veh/km ∗ l, $Q_{main} = 1868$ veh/h ∗ l, a fuzzy boundary $Q_{in} = 1000$ veh/h ∗ l is found. When the merging traffic volume is less than 1000 veh/h ∗ l, traffic condition in the intersected road is only affected by lane-changing behaviors. When the merging traffic volume is larger than 1000 veh/h ∗ l, traffic condition in the intersected road would be affected by the exceeding HNAC. This result corresponds to the theoretical analysis in Section 3.2, moreover, providing a fuzzy value of HNAC in a specific background traffic condition. In all of the 110 simulation groups in this study, the fuzzy boundary in every group could be found. However, to determine the explicit equation of HNAC, some further studies are still needed.

6.2. Standard Deviation and Correlation Coefficient Analysis. From the analysis in Section 6.1, it could be known that with the increasing of merging traffic volume, velocity dispersion in intersected road also increased gradually. When exceeding the fuzzy boundary (HNAC), velocity dispersion in on-ramp shows a steep increase and the synchronization also appears. In mathematical language, standard deviation (Std) of the traffic velocity in intersected road is increasing with merging traffic volume. In a moment around the steep increase point, Std from the intersected road will equal to that from

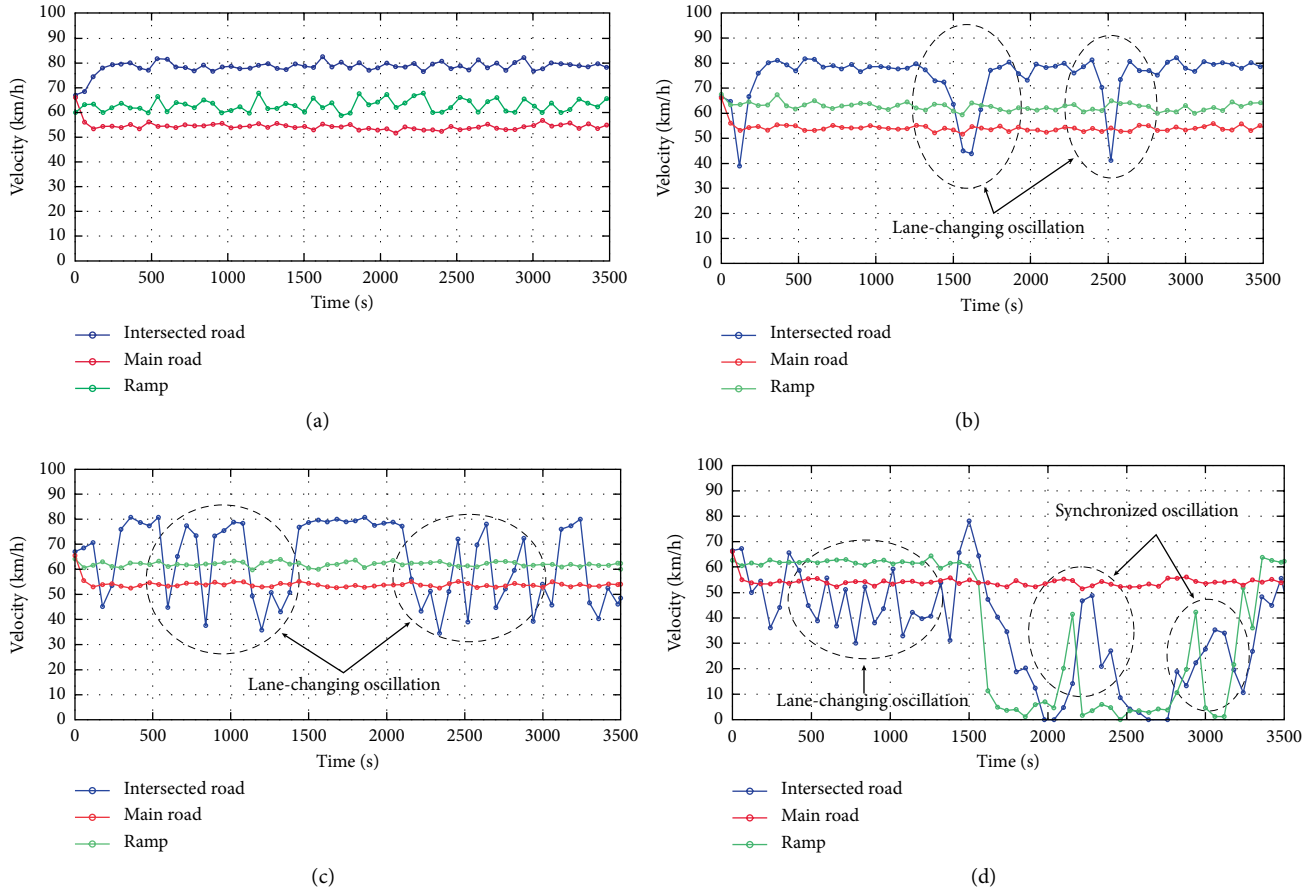

FIGURE 8: The data examples analysis. (a) $Q_{main} = 1868$ veh/h $*$ l, $Q_{in} = 100$ veh/h $*$ l, (b) $Q_{main} = 1868$ veh/h $*$ l, $Q_{in} = 300$ veh/h $*$ l, (c) $Q_{main} = 1868$ veh/h $*$ l, $Q_{in} = 700$ veh/h $*$ l, (d) $Q_{main} = 1868$ veh/h $*$ l, $Q_{in} = 1000$ veh/h $*$ l.

on-ramp, caused by synchronization. Moreover, the synchronization could be expressed by correlation coefficient. When merging traffic volume is less than the boundary (HNAC), the coefficient remains in a relatively low level, and when the merging traffic volume is larger than HNAC, the coefficient remains in a high level.

In this part, Std σ is calculated by equation (23), and Spearman correlation coefficient (ρ) (SCC) is adopted because it is suitable to randomly distributed data set, calculated by equation (24).

$$\sigma = \sqrt{\frac{\sum (x - \overline{x})^2}{n}}, \tag{23}$$

$$\rho = \frac{\sum_{i=1}^{N} (x_i - \overline{x})(y_i - \overline{y})}{\sqrt{\sum_{i=1}^{N} (x_i - \overline{x})^2 \sum_{i=1}^{N} (y_i - \overline{y})^2}}. \tag{24}$$

Taking the data test groups of $r = 10\%$ as examples, $k_{main} \in [30, 66]$(veh/km $*$ 1), Q_{main} is calculated by equation (22). The total number of simulation groups of $r = 10\%$ is 10, and information concluded from each simulation group is basically of same kind. Therefore, there is no need to list all the simulation results. Std and SCC in group $v_{main} = 54.9$ km/h, $Q_{main} = 1868$ veh/h $*$ l, $Q_{in} \in [100, 1800]$veh/h $*$ l and group $v_{main} = 28.3$ km/h, $Q_{main} = 1414$ veh/h $*$ l, $Q_{in} \in [100, 1400]$ veh/h $*$ l are chosen as presentations, shown in Figure 9.

In these figures, trends of Std in intersected road traffic velocity and on-ramp velocity are depicted in upper parts. SCCs between intersected road traffic velocity and on-ramp velocity are depicted in lower parts. From the figures shown above, discontinuity point of Std and SCC implies a same fuzzy boundary (HNAC) of the merging traffic volume. In left side of this point, both Std and SCC stayed in a very low stable value. In right side of this point, they stayed in a relatively high stable value. It could be seen in upper parts that there exists a point where the Std of the intersected road traffic velocity equals to that in on-ramp. This could provide us the accurate value of the fuzzy boundary (HNAC). Moreover, with the value of Q_{main} decreased, which means the traffic condition of the main road became more severe, the fuzzy boundary (HNAC) also went down, corresponding to the theoretical result in Section 4.2.

6.3. The Explicit Equation of HNAC. From Figure 9, the point where Std of intersected road traffic velocity equals to that in on-ramp refers to the accurate value of the fuzzy boundary (HNAC). In that, 10 HNAC values could be obtained in different traffic conditions of the main road, when heavy vehicle mixing ratio equals to 10%. Therefore, 110 HNAC values in traffic stream of different heavy vehicle mixing ratios

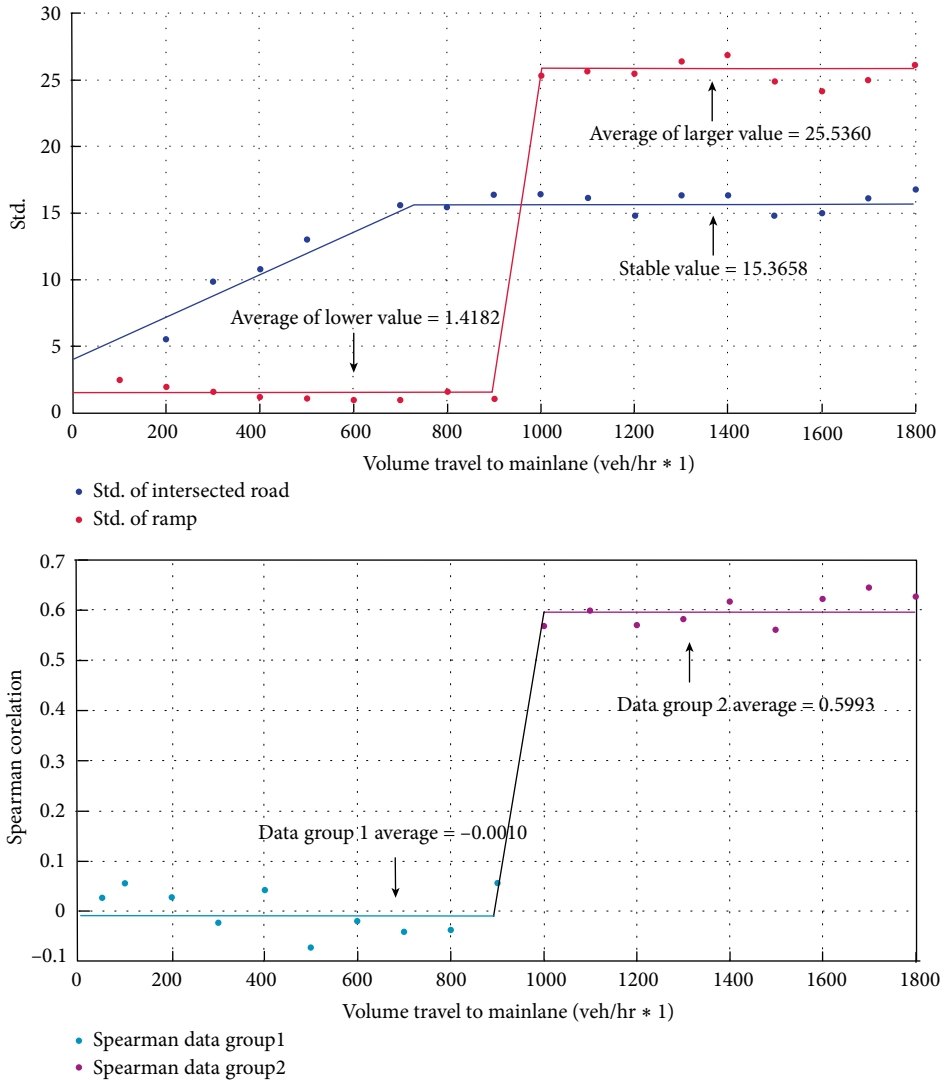

(a)

Figure 9: Continued.

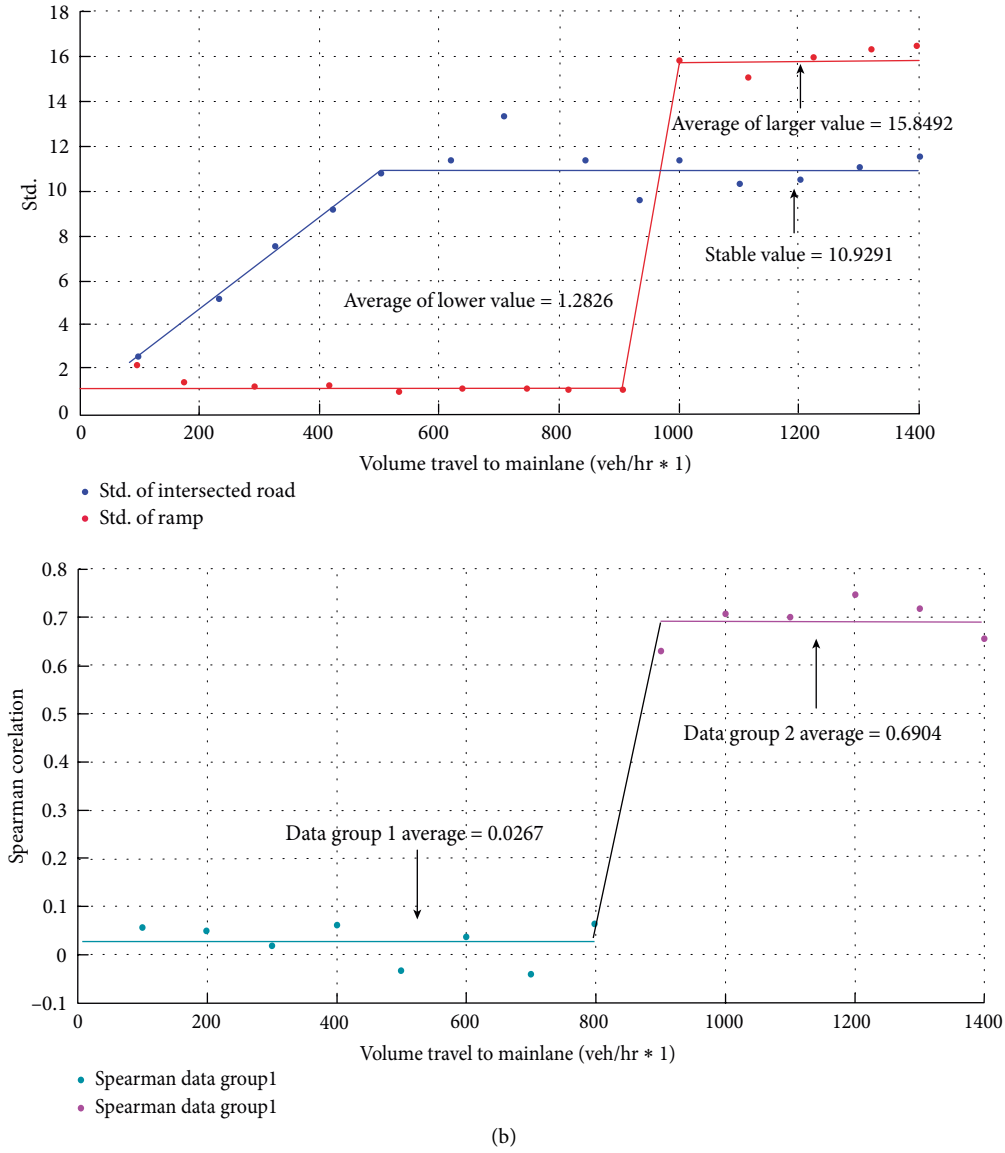

(b)

FIGURE 9: Std and SCC when $r = 10\%$, taking two simulation groups for presentation.

Table 2 and different main road's traffic conditions could be obtained. The theoretical conclusion in Section 4.2 that HNAC is linear positive correlated to traffic volume of the main road Q_{main} has been proved by simulation data. With our previous work [1], the traffic volume is also linearly related to heavy vehicle mixing ratio r. Thus, the assumption of the explicit equation of HNAC could be reasonably presented as below.

$$\text{HNAC} = f(Q_{\text{main}}, r) = \varphi(r)Q_{\text{main}} + \omega(r), \tag{25}$$

$$\varphi(r) = p_1 r + p_2, \tag{26}$$

$$\omega(r) = p_1' r + p_2'. \tag{27}$$

Using the 110 HNAC values obtained in Section 6.2 to linear fit equation (25), the result is shown in Figure 10. The values of $\varphi(r)$ and $\omega(r)$ in traffic conditions with different r values are also obtained, provided in Table 3.

From the linear fitting results given above, the explicit equation of relationship (26) and (27) could be obtained. The values of Adj $- R^2$ have proved the accuracy of linear fitting. Therefore, the explicit equation of HNAC is shown below.

$$\varphi(r) = 0.68r + 0.2, \tag{28}$$

$$\omega(r) = -690r + 93, \tag{29}$$

$$\text{HNAC} = f(Q_{\text{main}}, r) = 0.68Q_{\text{main}} \cdot r + 0.2Q_{\text{main}} - 690r + 93. \tag{30}$$

6.4. Model Validation. Following the explicit equation of HNAC obtained in Section 6.3, model validation is provided in this part. As depicted in Section 1, HNAC is defined as the upper limit of traffic volume merging into main road through the on-ramp. If this value was exceeded by merging volume, the traffic flow of intersected road will be affected. To validate the model, traffic dynamic should be supervised in a certain highway node, including real time variance of traffic volume and velocity in main road, intersected road and on-ramp. When the oscillation

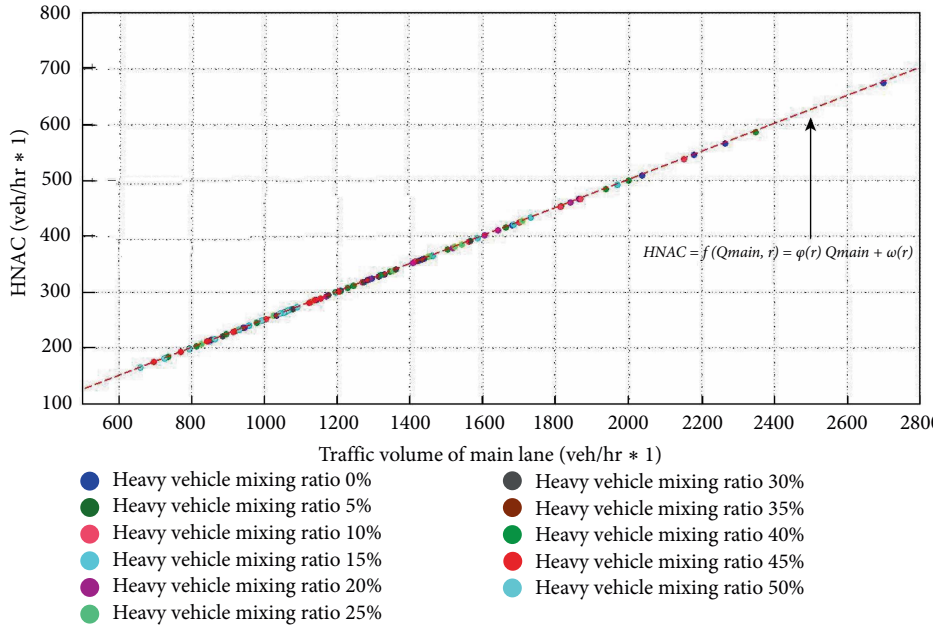

Figure 10: Linear fit of equation (25).

mentioned in Section 6.1 happens, merging volume should be recorded and compared to theoretical HNAC obtained from equation (30), to verify the accuracy of the model.

In order to prove the accuracy of HNAC model introduced in this article, Maoerliu interchange of Xi'an Ring Expressway (G3001) was chosen as the supervision objective. Taking northbound section as the main road, and westbound as the intersected road, detectors were deployed as shown in Figure 11. Besides, all detectors have avoided the merging and diversion areas, to reduce the impact of weaving traffic. Traffic volume and velocity of the three detection points were supervised during 2019.09.15–2019.09.26.

In field detection, the oscillation mentioned in previous could only be caught in peak hours, and 28 oscillations in intersected road caused by exceeding HNAC were observed. From equation (30), it is known that HNAC varied with traffic volume and heavy vehicle mixing ratio (r) in main road. In selected part of G3001, r remains in about 12–14%, taking 13% as average, the HNAC distribution curve could be obtained. Moreover, merging volume and traffic volume of 28 oscillations were collected. Comparing the theoretical values with the supervised values, the accuracy of the model could be observed, shown in Figure 12.

From Figure 12, it can be seen, 28 supervised HNACs spread around the theoretical curve obtained from equation (30), basically in range of [1100, 1650]veh/h * l. The distribution of 28 supervised HNACs is random and homogeneous, and the average relative error of supervised HNACs is 14.6%, which is an acceptable level, proving the accuracy of the model introduced in this article. Moreover, owning to the lack of related studies, it is unfortunately that the model in this paper could not be compared to other similar ones.

7. Discussion and Conclusions

The purpose of building microscopic model is not complex. The first one is to analyze the cause of HNAC in microscopic method. Another is to determine the boundary condition of merging to targeted lane under the dimension of space, which could be used as an intermediate variable in macroscopic modelling. It should be declared that the microscopic merging process is simplified, by bypassing the process of deceleration or acceleration of the merging vehicle. Compared to related works, this consideration largely reduced the complexity of microscopic modelling based on lane-changing rules. Moreover, the microscopic explain of traffic oscillations, the result of macroscopic model in Section 4.2, and data simulation also proved its rationality. The macroscopic model of HNAC is built using the boundary condition mentioned above. Macroscopic models were built in congested flow and free flow based on different assumptions respectively, providing the function of HNAC and also explained the production of oscillations. And this is an advantage which made it stay closer to actual traffic situations. Besides, it provided a thought of connecting microscopic problem and macroscopic problem.

The data simulation method is chosen instead of field data because it is difficult to collect enough real road data with different heavy vehicle mixing ratios and merging traffic volume in one specific highway node. Therefore, the simulation model is built based on rigid car-following behaviors organization and also controlled by macroscopic traffic flow model, to guarantee not only the typical traffic flow phenomenon such as oscillations and traffic waves, but also the comprehensive background traffic condition needed in this paper. However, it should be noticed, driving characters were simplified and idealized in theoretical models, and for instance, vehicle acceleration and deceleration processes were neglected. This might cause some differences. From Figure 8 in Section 6.1, though synchronization phenomenon could be significantly observed, lines depicting velocity in on-ramp and intersected road were not closely matched, and volatility of velocity curves were obvious. This phenomenon was mainly caused by the gap between theoretical models and real traffic conditions represented by simulation. Furthermore, from Figure 10 and Table

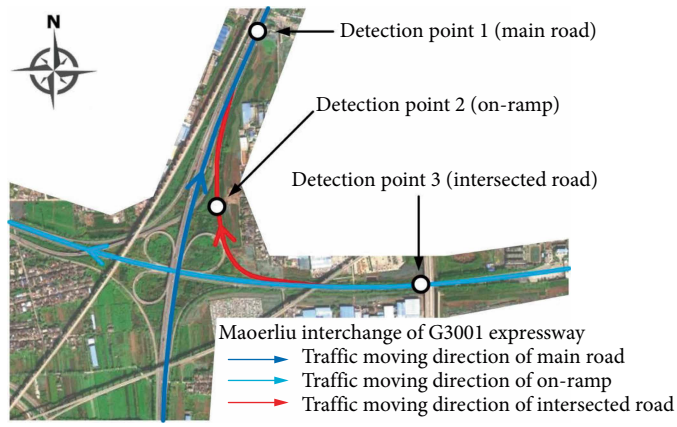

Figure 11: Maoerliu interchange of G3001 and the detectors deployment.

Table 3: The values of $\varphi(r)$ and $\omega(r)$.

r (%)	$\varphi(r)$	$\omega(r)$	Adj $- R^2$
0%	0.2155	89.82	0.9641
5%	0.2475	57.93	0.9674
10%	0.2747	23.35	0.9711
15%	0.3004	−9.10	0.9736
20%	0.3213	−36.68	0.9737
25%	0.3517	−77.48	0.9683
30%	0.3850	−108.80	0.9697
35%	0.4372	−162.40	0.9558
40%	0.4652	−181.20	0.9511
45%	0.5131	−215.70	0.9473
50%	0.5692	−252.00	0.9443

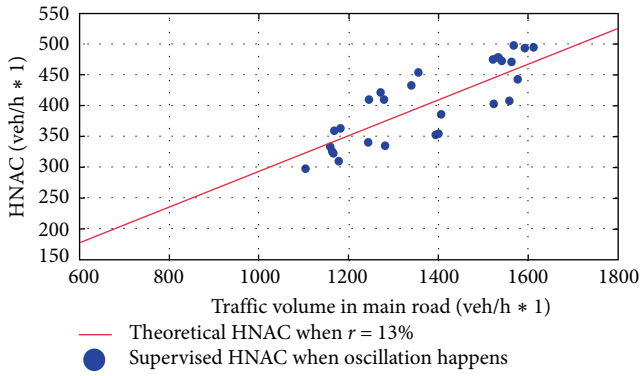

Figure 12: Comparison between theoretical HNAC and supervised values.

3 provided in Section 6.3, accuracy obtained from simulation data were significantly higher than that from the field test, depicted in Figure 12. This might be caused by ignorance of timid and aggressive drivers mentioned in Section 4. When timid drivers took the majority part of on-ramp traffic flow, they might lose some opportunities of merging into the traffic flow in main road, and HNAC of this situation might be smaller than theoretical value. Points below theoretical curve in Figure 12 stand for the situation mentioned above, and points above the curve represent the opposite situation. Unfortunately, accsurate number or proportion of timid and aggressive drivers could not be obtained. Therefore, to make HNAC more accurate and practical, large amount of real traffic data are needed, including detailed information of drivers in real road, geometric conditions, roadside facilities and traffic rules.

The definition of HNAC provided in Section 1 has implied that this concept lies in the macroscopic aspect, which is more related to a specific highway node than a road section. This concept derived from a simple observation towards the traffic condition of a specific highway node, and it is very likely to be noticed by other researchers. However, directly related works were not found, owning to the contribution of car-following models and moving bottleneck theory, which provide sufficient and efficient methods to solve many important existing traffic problems, lane-changing behaviours, traffic oscillations and breakdown, stop-and-go waves, relaxation phenomenon, etc. But, moving the consideration to large scale macroscopic problems, especially the propagation mechanism of traffic emergencies on highway network, which is very helpful to large scale evacuation and rescue, the systematic research of HNAC becomes important. In policy and planning aspects, when an emergency happens downstream a highway node, the traffic condition in road section could be obtained through kinetic wave models. In this situation, if the traffic volume in on-ramp exceeded HNAC of the main road, congestion will form in on-ramp and further affects the traffic flow in intersected road, meaning that the emergency effect will spread into the intersected road. Based on the judgement mentioned above, the approximate range of emergency effect in road network could be obtained, providing a base line to traffic management departments in dealing traffic emergency.

Data Availability

Data in this article are available only with permission of corresponding author.

Conflicts of Interest

The authors declare that they have no conflicts of interest.

References

[1] X. Liu, J. Xu, M. Li, L. Wei, and H. Ru, "General-logistic-based speed-density relationship model incorporating the effect of heavy vehicles," *Mathematical Problems in Engineering*, vol. 2019, Article ID 6039846, 10 pages, 2019.

[2] C. F. Daganzo, "The cell transmission model, part II: network traffic," *Transportation Research Part B: Methodological*, vol. 29, no. 2, pp. 79–93, 1995.

[3] B. S. Kerner, "Three phase traffic theory and highway capacity," *Physica A: Statistical Mechanics and its Applications*, vol. 333, no. 379, pp. 440–440, 2004.

[4] B. S. Kerner and S. L. Klenov, "Phase transitions in traffic flow on multilane roads," *Physical Review E*, vol. 80, no. 5, 2009.

[5] B. S. Kerner, S. L. Klenov, and M. Schreckenberg, "Probabilistic physical characteristics of phase transitions at highway bottlenecks: incommensurability of three-phase and two-phase traffic-flow theories," *Physical Review E*, vol. 89, no. 5, Article ID 052807, 2014.

[6] B. S. Kerner, "Microscopic theory of traffic flow instability governing traffic breakdown at highway bottlenecks: growing wave of increase in speed in synchronized flow," *Physical Review E*, vol. 92, no. 6, 2015.

[7] X. J. Hu and M. Y. Liu, "Traffic flow in the vicinity of crosswalks on a provincial highway in China," *Modern Physics Letters B*, vol. 32, no. 31, Article ID 1850378, 2018.

[8] X. Hu, F. Zhang, J. Lu, M. Liu, Y. Ma, and Q. Wan, "Research on influence of sun glare in urban tunnels based on cellular automaton model in the framework of Kerner's three-phase traffic theory," *Physica A: Statistical Mechanics and its Applications*, vol. 527, Article ID 121176, 2019.

[9] G. F. Newell, "A simplified car-following theory: a lower order model," *Transportation Research Part B: Methodological*, vol. 36, no. 3, pp. 195–205, 2002.

[10] L. A. Pipes, "An operational analysis of traffic dynamics," *Journal of Applied Physics*, vol. 24, no. 3, pp. 274–281, 1953.

[11] E. Kometani and T. Sasaki, "On the stability of traffic flow," *Journal of the Operations Research Society of Japan*, vol. 2, no. 1, pp. 11–26, 1958.

[12] E. Kometani and T. Sasaki, *Dynamic Behavior of Traffic with a Nonlinear Spacing-Speed Relationship*, Elsevier, Amsterdam, 1961.

[13] D. C. Gazis, R. Herman, and R. W. Rothery, "Nonlinear follow-the-leader models of traffic flow," *Operations Research*, vol. 9, no. 4, pp. 545–567, 1961.

[14] J. M. Castillo and F. G. Benitez, "On the functional form of the speed-density relationships I: general theory," *Transportation Research Part B*, vol. 29, no. 5, pp. 373–406, 1995.

[15] B. S. Kerner and H. Rehborn, "Experimental features and characteristics of traffic jams," *Physical Review E*, vol. 53, no. 2, pp. R1297–R1300, 1996.

[16] H. Wei, E. Meyer, J. Lee, and C. Feng, "Characterizing and modeling observed lane-changing behavior: lane-vehicle-based microscopic simulation on urban street network," *Transportation Research Record: Journal of the Transportation Research Board*, vol. 1710, no. 1, pp. 104–113, 2000.

[17] S. L. Cohen, "Application of relaxation procedure for lane changing in microscopic simulation models," *Transportation Research Record: Journal of the Transportation Research Board*, vol. 1883, no. 1, pp. 50–58, 2004.

[18] J. A. Laval and L. Leclercq, "Microscopic modeling of the relaxation phenomenon using a macroscopic lane-changing model," *Transportation Research Part B: Methodological*, vol. 42, no. 6, pp. 511–522, 2008.

[19] L. Leclercq, N. Chiabaut, J. A. Laval, and C. Buisson, "Relaxation phenomenon after lane changing," *Transportation Research Record: Journal of the Transportation Research Board*, vol. 1999, no. 1, pp. 79–85, 2007.

[20] A. Duret, S. Ahn, and C. Buisson, "Passing rates to measure relaxation and impact of lane-changing in congestion," *Computer-Aided Civil and Infrastructure Engineering*, vol. 26, no. 4, pp. 285–297, 2011.

[21] J. A. Laval, "Linking synchronized flow and kinematic wave theory," *Traffic and Granular Flow*, pp. 521–526, Springer, Berlin, 2005.

[22] J. A. Laval and C. F. Daganzo, "Lane-changing in traffic streams," *Transportation Research Part B: Methodological*, vol. 40, no. 3, pp. 251–264, 2006.

[23] S. Ahn and M. Cassidy, "Freeway traffic oscillations and vehicle lane-change manoeuvres," *Transportation and Traffic Theory 2007*, pp. 691–710, London, Emerald Group Publishing Limited, 2007.

[24] J. A. Laval and L. Leclercq, "A mechanism to describe the formation and propagation of stop-and-go waves in congested freeway traffic," *Philosophical Transactions of the Royal Society A: Mathematical, Physical and Engineering Sciences*, vol. 368, no. 1928, pp. 4519–4541, 2010.

[25] D. Chen, J. Laval, Z. Zheng, and S. Ahn, "A behavioral car-following model that captures traffic oscillations," *Transportation Research Part B: Methodological*, vol. 46, no. 6, pp. 744–761, 2012.

[26] D. Chen, S. Ahn, and A. Hegyi, "Variable speed limit control for steady and oscillatory queues at fixed freeway bottlenecks," *Transportation Research Part B: Methodological*, vol. 70, pp. 340–358, 2014.

[27] D. Chen and S. Ahn, "Variable speed limit control for severe non-recurrent freeway bottlenecks," *Transportation Research Part C*, vol. 51, pp. 210–230, 2015.

[28] Y. Han and S. Ahn, "Stochastic modeling of breakdown at freeway merge bottleneck and traffic control method using connected automated vehicle," *Transportation Research Part B: Methodological*, vol. 107, pp. 146–166, 2018.

[29] P. G. Gipps, "A model for the structure of lane-changing decisions," *Transportation Research Part B: Methodological*, vol. 20, no. 5, pp. 403–414, 1986.

[30] D. Chowdhury, D. E. Wolf, and M. Schreckenberg, "Particle hopping models for two-lane traffic with two kinds of vehicles: effects of lane-changing rules," *Physica A: Statistical Mechanics and its Applications*, vol. 235, no. 3-4, pp. 417–439, 1997.

[31] K. Nagel, D. E. Wolf, P. Wagner, and P. Simon, "Two-lane traffic rules for cellular automata: a systematic approach," *Physical Review E*, vol. 58, no. 2, pp. 1425–1437, 1998.

[32] P. Wagner, K. Nagel, and D. E. Wolf, "Realistic multi-lane traffic rules for cellular automata," *Physica A: Statistical Mechanics and its Applications*, vol. 234, no. 3-4, pp. 687–698, 1997.

[33] P. Hidas, "Modelling lane changing and merging in microscopic traffic simulation," *Transportation Research Part C: Emerging Technologies*, vol. 10, no. 5-6, pp. 351–371, 2002.

[34] J. A. Laval, "Stochastic processes of moving bottlenecks: approximate formulas for highway capacity," *Transportation Research Record: Journal of the Transportation Research Board*, vol. 1988, no. 1, pp. 86–91, 2006.

[35] A. Kesting, M. Treiber, and D. Helbing, "General lane-changing model MOBIL for car-following models," *Transportation Research Record: Journal of the Transportation Research Board*, vol. 1999, no. 1, pp. 86–94, 2007.

[36] D. C. Gazis and R. Herman, "The moving and "Phantom" bottlenecks," *Transportation Science*, vol. 26, no. 3, pp. 223–229, 1992.

[37] C. F. Daganzo and J. A. Laval, "On the numerical treatment of moving bottlenecks," *Transportation Research Part B: Methodological*, vol. 39, no. 1, pp. 31–46, 2005.

[38] J. C. Munoz and C. F. Daganzo, "Moving bottlenecks: a theory grounded on experimental observation," *Transportation and Traffic Theory in the 21st Century*, pp. 441–461, Bingley, West Yorkshire, England, Emerald Group Publishing Limited, 2004.

[39] B. S. Kerner and S. L. Klenov, "A theory of traffic congestion at moving bottlenecks," *Journal of Physics A: Mathematical and Theoretical*, vol. 43, no. 42, p. 425101, 2010.

[40] H. Wang, J. Li, Q. Chen, and D. Ni, "Logistic modeling of the equilibrium speed-density relationship," *Transportation Research Part A: Policy and Practice*, vol. 45, no. 6, pp. 554–566, 2011.

[41] F. Huang, P. Liu, H. Yu, and W. Wang, "Identifying if VISSIM simulation model and SSAM provide reasonable estimates for field measured traffic conflicts at signalized intersections," *Accident Analysis and Prevention*, vol. 50, pp. 1014–1024, 2013.

[42] T. Hu, "Calibration of microscopic traffic simulation model for weaving sections expressway," Beijing Jiaotong University, 2010.

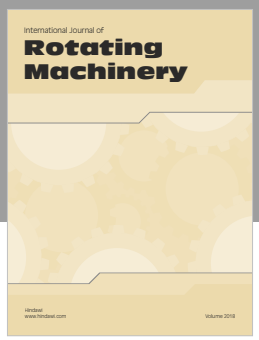

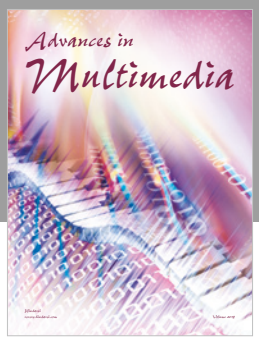

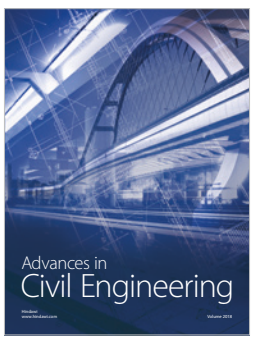

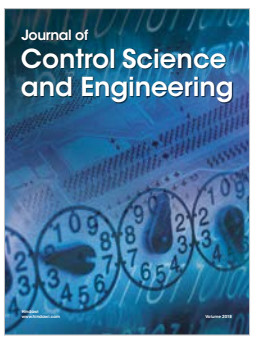

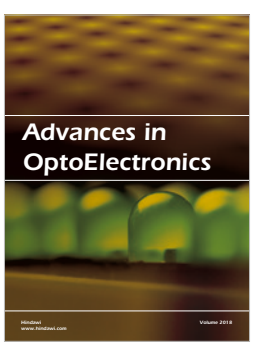

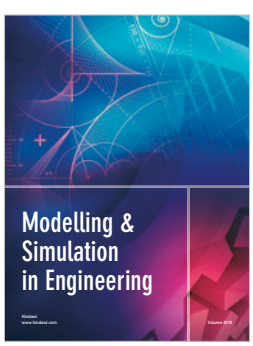

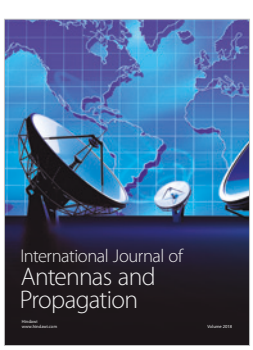

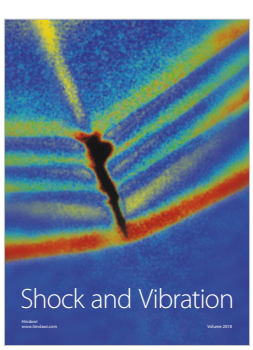

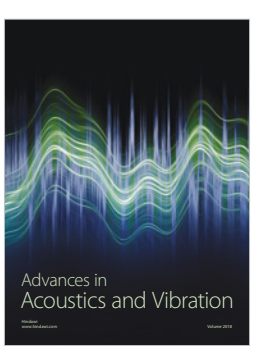

Hindawi

Submit your manuscripts at
www.hindawi.com